Nuclear effects on the eigenvalues of the $dt\mu$ molecule

Michael C. Struensee, G. M. Hale, Russell T Pack, and James S. Cohen
Theoretical Division, Los Alamos National Laboratory, Los Alamos, New Mexico 87545
(Received 1 June 1987)

The latest information about the ^{5}He nuclear system in terms of R-matrix parameters has been matched to adiabatic $dt\mu$ molecular wave functions in order to determine the complex eigenvalues of the molecule. Through the use of the reduced R-matrix formalism, the matching is accomplished by considering only the $L=0$ $dt\mu$ states explicitly. These states are calculated in a series of increasingly more accurate adiabatic approximations that, at least for the lowest vibrational level, appear to be converging to the exact nonadiabatic result. The best complex eigenvalues thus obtained probably have less than 10% uncertainty, and are in reasonably good agreement with those of Bogdanova *et al.* (Zh. Eksp. Teor. Fiz. **81**, 829 (1981) [Sov. Phys.—JETP **54**, 442 (1981)]).

I. INTRODUCTION

Nuclear effects on the properties of the $dt\mu$ molecule have received increased attention recently because of intriguing experimental results[1] concerning the sticking of muons to α particles that cannot be entirely explained by conventional calculations.[2] The first step in assessing nuclear effects is to calculate their perturbation of the molecular binding energies and wave functions. Such calculations were reported a few years ago by Bogdanova and co-workers,[3,4] using a generalized optical-potential approach to account for the nuclear reactions, and approximate methods to find the width Γ and position E_r of the resonance that corresponds to the complex eigenvalue $E_0=E_r-i\Gamma/2$.

Here we report a calculation that uses an R-matrix parametrization of the five-nucleon interactions at short distances, and searches in the complex energy plane for a match to the purely outgoing-wave molecular solution, obtained in the adiabatic approximation, in order to determine the complex eigenvalue directly. Despite significant differences in the formulation of the problem and in the calculational methods and numerical input used, we obtain answers that are close to those of Bogdanova *et al.*[4]

Our approach is based on the usual R-matrix separation of coordinate space. Outside of a relatively small region which we call the "nuclear region," the five nucleons are assumed to coalesce into fragment pairs ($d+t$ and $n+\alpha$) between which no short-ranged nuclear forces act. Since reliable microscopic calculations of the five-nucleon wave function are not yet available, we use a phenomenological R-matrix parametrization of the wave function on the nuclear surface that encloses the nuclear region. This parametrization is described in Sec. II. Predictably, the effect of the muon in this region is small, showing up approximately as a slight shift in the energy levels of the R matrix.

In the "channel region" outside of the nuclear surface, only long-ranged Coulomb forces can act pairwise between the fragments, and between the muon and the fragments. Here, the Coulomb attraction of the muon is quite important, being most evident in the $dt\mu$ channel, where it causes molecular bound states to occur. We have used a sequence of progressively more accurate adiabatic approximations to solve the $dt\mu$ Coulomb problem. These include the Born-Oppenheimer, standard adiabatic, and improved adiabatic approximations, which are described in Sec. III.

In conventional $dt\mu$ molecular bound-state calculations the nuclear region is ignored, and the $dt\mu$ channel region includes the origin. In the two-region approach we are using, the left-hand boundary conditions of regularity at the origin are replaced by continuity conditions at the nuclear surface. As a result of these left-hand nuclear boundary conditions, the asymptotic solution in the channel region, $\Psi\sim-\mathcal{I}+\mathcal{O}S$, contains both incoming ($\mathcal{I}$) and outgoing ($\mathcal{O}$) waves, with relative amplitudes given by elements of the S matrix. The generalization of the bound-state asymptotic (right-hand) boundary condition of exponential decay is the purely outgoing-wave condition, which corresponds to a pole of the S matrix at the complex eigenvalue E_0. The determination of the complex eigenvalue is described in Sec. IV as a variation of the conventional single-region bound-state calculation. Numerical values of E_0 are tabulated for each of the adiabatic approximations used, along with the results of Bogdanova *et al.*[4] In the concluding remarks of Sec. V, we compare numerical results of the various calculations, discuss the differences between our methods and those of Bogdanova *et al.*, and make estimates of the uncertainty of our eigenvalue calculations.

II. THE NUCLEAR REGION

A. ^{5}He$+\mu$ system R matrix

We write the total Hamiltonian for the ^{5}He$+\mu$ system in the nuclear region as

$$H=H_N(\{\mathbf{x}_N\})+H_\mu(\mathbf{r}_\mu,\{\mathbf{x}'_N\})\ , \tag{1}$$

where $\{\mathbf{x}_N\}$ is a complete set of nuclear coordinates and $\mathbf{r}_\mu$ is the muon coordinate relative to the five-nucleon center of mass, and $\{\mathbf{x}'_N\}$ is a reduced set of nuclear coordinates that refers only to the protons. When the nucleons are close enough together to experience nuclear forces, the coordinates $\{\mathbf{x}'_N\}$ will generally be negligible compared to $\mathbf{r}_\mu$ and

$$H \approx H_N(\{\mathbf{x}_N\}) + H_\mu(\mathbf{r}_\mu) \tag{2}$$

becomes approximately separable with solution

$$\Psi \approx \psi_N(\{\mathbf{x}_N\})\phi_\mu(\mathbf{r}_\mu) \ . \tag{3}$$

At energies in the vicinity of the $dt\mu$ molecular ground state, contributions to ψ_N from continuum states are important because n-α scattering is open below the d-t threshold, and the effects of the $J^\pi = \frac{3}{2}^+$ resonance just above the threshold extend to energies below it. R-matrix theory[5] provides a convenient framework for a phenomenological description of the surface properties of the wave function, while at the same time discretizing the continuum. We therefore expand ψ_N inside the nuclear region in terms of the solutions of

$$(H_N + \mathcal{L}_B - E_\lambda)\,|\,\lambda) = 0 \ , \tag{4}$$

in which $\mathcal{L}_B$ is the Bloch operator that imposes boundary conditions B on the logarithmic derivative of the wave function at the nuclear surface (sometimes also called the "channel" surface). The muon energies, on the other hand, are sufficiently low that we approximate the muon state with the ground-state wave function, $\phi^0_\mu(\mathbf{r}_\mu)$, satisfying

$$(H_\mu - E^0_\mu)\phi^0_\mu(\mathbf{r}_\mu) = 0 \ , \tag{5}$$

for the muon orbiting ^{5}He. This assumption joins smoothly with the adiabatic approximations that are used in the $dt\mu$ channel region for the problem, described in Sec. III A.

One can define the R matrix (including the muon) for the nuclear region by taking channel-surface projections of the Green's function $G = (H + \mathcal{L}_B - E)^{-1}$ for the system at total center-of-mass (c.m.) energy E,

$$R_{c'c} = (c'\,|\,G\,|\,c) = |\,\phi^0_\mu)(\phi^0_\mu\,|\sum_\lambda \frac{\gamma_{c'\lambda}\gamma_{c\lambda}}{E_\lambda + E^0_\mu - E} \ . \tag{6}$$

The channel-surface functions,

$$(\mathbf{r}_c\,|\,c) = \left[\frac{1}{2M_c a_c}\right]^{1/2} \frac{\delta(r_c - a_c)}{r_c}$$

$$\times [(\phi_1 \otimes \phi_2)_{sv} \otimes i^l Y_{lm}(\hat{\mathbf{r}}_c)]_{JM} \ , \tag{7}$$

are defined (in units such that $\hbar = e = 1$) at channel radii a_c for the (two-body) channels of the nuclear system ($d+t$ and $n+\alpha$) in terms of the channel reduced masses M_c, radial coordinates $\mathbf{r}_c$ (i.e., $\mathbf{r}_{dt}$ and $\mathbf{r}_{n\alpha}$ in Fig. 1), spin-dependent bound-state fragment wave functions ϕ_1 and ϕ_2 that couple to channel spin s with projection v, and spherical harmonics Y_{lm} that then couple to total angular momentum J with projection M. The reduced-width amplitudes $\gamma_{c\lambda}$ are the channel-surface projections $(c\,|\,\lambda)$.

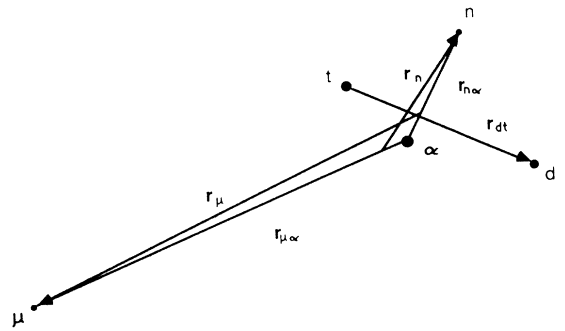

FIG. 1. Coordinates for describing the channel region of ^{5}He$+\mu$. Radii with two subscripts are interparticle separation coordinates; those with single subscripts are relative to the center of mass of the remaining pair.

An R-matrix analysis of the reactions in the ^{5}He system determines for boundary conditions B_c and channel radii a_c the parameters $\gamma_{c\lambda}$ and E_λ that, together with the ground-state energy and wave function for μ-^{5}He, completely specify the R-matrix elements of Eq. (6). Such an analysis[6] has been completed recently for ^{5}He at excitation energies up to 21.5 MeV. The parameters relevant to this calculation are those for total angular momentum and parity $J^\pi = \frac{3}{2}^+$, in which the famous nuclear resonance occurs. (The $J = \frac{1}{2}$ S-wave transition contributes $\sim 1\%$ to the nuclear reaction at low energies.) These have been given in Ref. 7, but we repeat them here in Table I for convenient referral.

B. $dt\mu$ reduced R matrix

Our method uses continuity of the logarithmic derivatives of the wave function (essentially the reciprocal of the R matrix) across the nuclear surface, which implies matching to both $dt\mu$ and $n\alpha\mu$ channels. However, the matching is done explicitly only in the S-wave $dt\mu$ channel, using a partitioned matrix technique called the reduced R matrix.[8] This technique makes use of the fact that for incoming S waves in the $dt\mu$ channel there are only outgoing waves in the other channels having known logarithmic derivatives at the nuclear surface.

Let us split the four channels listed in Table I so that channel $1 = {}^4S(dt)$ is separated out and the remaining three, $2 = {}^4D(dt)$, $3 = {}^2D(dt)$, and $4 = {}^2D(n\alpha)$, are grouped together in partition "Q." Then the channel-1 reduced R-matrix element,

$$\tilde{R}_1 = R_{11} + R_{1Q}(L_Q - B_Q)[1 - R_{QQ}(L_Q - B_Q)]^{-1}R_Q \ , \tag{8}$$

involves all the elements of R, as well as the outgoing-wave logarithmic derivatives L_Q for the channels in partition Q. According to our separable approximation, Eq.

TABLE I. R-matrix parameters for the $J^{\pi}=\frac{3}{2}^{+}$ of ^{5}He. Channel labels (c) are in spectroscopic notation. Eigenenergies E_λ are center-of-mass values in MeV relative to the d-t threshold; reduced-width amplitudes $\gamma_{c\lambda}$ are also center of mass in units MeV$^{1/2}$.

$c\,(J=\frac{3}{2})$	a_c(fm)	B_c	$\lambda=1$	$\lambda=2$	$\lambda=3$	$\lambda=4$
				E_λ		
			0.083 755 9	6.471 304 3	13.735 706 7	47.475 246
				$\gamma_{c\lambda}$		
$^4S(dt)$	5.1	−0.37	1.176 067 8	0.069 339 7	−0.495 543 8	1.105 242 1
$^4D(dt)$	5.1	−2.00	0.168 872 4	−0.272 980 5	1.991 068 1	1.984 704 8
$^2D(dt)$	5.1	−2.00	−0.048 479 7	0.886 247 5	0.095 851 3	0.242 246 4
$^2D(n\alpha)$	3.0	−0.59	0.376 821 8	−0.156 273 7	0.999 449 4	−3.855 653 9

(3), the outgoing-wave logarithmic derivatives in the Q channels are given by

$$L_c=a_c\frac{\partial}{\partial r_c}\mathcal{O}_c(k_c,r_c)/\mathcal{O}_c(k_c,r_c)\Big|_{r_c=a_c}, \tag{9}$$

for $c=2,3,4$, where $\mathcal{O}_c$ is the spherical outgoing (Coulomb) wave and k_c is the c.m. wave number (momentum) in channel c. A justification of the separable approximation in the $n\alpha\mu$ channel and the relation of its channel momentum to that of the $dt\mu$ channel are given in Sec. III B. The quantity

$$\tilde{L}_1=\frac{1}{\tilde{R}_1}+B_1 \tag{10}$$

gives the boundary value at the nuclear surface of the effective logarithmic derivative of the radial S-wave d-t wave function inside the nuclear region, which serves as the matching condition for the $dt\mu$ wave function calculated in the channel region using the adiabatic approximation. Due to the energy dependence of the R-matrix elements and of the complex functions L_c, $\tilde{L}_1$ is, in general, complex and energy dependent. If the logarithmic derivatives of the solutions inside and outside the nuclear surface match for some complex energy E_0 at which the solution outside goes asymptotically to a pure outgoing wave, then

$$E_0=E_r-i\Gamma/2 \tag{11}$$

is a pole of the system S matrix, corresponding to a resonance at energy E_r with width Γ. Thus, the nuclear boundary condition $\tilde{L}_1$ changes the $dt\mu$ bound state into a resonance with $\Gamma\neq 0$, owing to the nonzero imaginary part of $\tilde{L}_1$ that comes even at real energies from the open n-α channel.

III. THE CHANNEL REGION

A. Adiabatic approximations for $dt\mu$

In the present work calculations have been substantially simplified by the replacement of the exact $dt\mu$ Schrödinger equation outside the nuclear region by an approximate Schrödinger equation. This reduction, called an adiabatic approximation, is achieved by taking the effect of the muon into account in an approximate way, through the introduction of a potential curve. Within the framework of adiabatic approximations, varying levels of accuracy may be obtained, depending upon the method of construction of the potential curves. For the current work, calculations have been performed which utilize the Born-Oppenheimer, standard adiabatic, and improved adiabatic methods of approximation.[9] This section contains a discussion of these methods and their application to the $dt\mu$ calculation.

The system of interest for this channel consists of the deuteron d, the triton t, and the muon μ interacting as point particles via the Coulomb interaction. For purposes of calculation, the respective masses have been taken to be $m_d=3670.481m_e$, $m_t=5496.918m_e$, and $m_\mu=206.768m_e$, where m_e is the mass of the electron. In general, the labeling of coordinates in the channel region will be that of Fig. 1. However, in order to avoid an abundance of subscripts when discussing the $dt\mu$ channel, we revert to the more conventional notation that $\mathbf{R}\equiv\mathbf{r}_{dt}$ is the relative d-t separation coordinate and $\mathbf{r}\equiv\mathbf{r}_\mu$ is the muon coordinate relative to the d-t (or n-α) center of mass. The nuclear reduced mass is given by $M_{dt}=m_dm_t/(m_d+m_t)$. After separating the center-of-mass motion, the exact $dt\mu$ Hamiltonian can be written as a sum of Born-Oppenheimer, internuclear orientation, internuclear separation, and mass polarization terms according to

$$H=H^{\mathrm{BO}}+H^{\mathrm{ang}}+H^{\mathrm{sep}}+H^{\mathrm{mp}}, \tag{12}$$

where

$$H^{\mathrm{BO}}=-\frac{1}{2m_\mu}\nabla_{\mathrm{r}}^2+\frac{1}{R}-\frac{1}{r_{d\mu}}-\frac{1}{r_{t\mu}}, \tag{13}$$

$$H^{\mathrm{ang}}=\frac{1}{2M_{dt}R^2}\mathbf{L}_{\mathrm{R}}^2, \tag{14}$$

$$H^{\mathrm{sep}}=-\frac{1}{2M_{dt}}\left[\frac{\partial^2}{\partial R^2}+\frac{2}{R}\frac{\partial}{\partial R}\right], \tag{15}$$

and

$$H^{\mathrm{mp}}=-\frac{1}{2(m_d+m_t)}\nabla_{\mathrm{r}}^2. \tag{16}$$

The energies and wave functions of the exact problem are obtained by solving the Schrödinger equation

$$H\Psi(\mathbf{r},\mathbf{R})=E\Psi(\mathbf{r},\mathbf{R}) \tag{17}$$

subject to the appropriate boundary conditions.

The main idea behind the adiabatic approximations is to approximate Eq. (17) by a pair of differential equations, each with fewer degrees of freedom than Eq. (17). This approach leads to considerable reduction in the effort required to obtain energies and wave functions. A brief description of the adiabatic procedures used for the current work is given below. For more details and derivations, the reader is referred to Ref. 9.

One method of implementing an adiabatic approximation is to partition the Hilbert space $\{\mathbf{r},\mathbf{R}\}$ of the original problem [Eq. (17)] into separate $\{\mathbf{r}\}$ and $\{\mathbf{R}\}$ spaces. Then the first stage of the procedure is carried out by solving the differential equation

$$H^{\mathrm{BO}}\phi_n(\mathbf{r};R)=E_n^{\mathrm{BO}}(R)\phi_n(\mathbf{r};R) \tag{18}$$

on the Hilbert space $\{\mathbf{r}\}$ for all values of the parameter R. In practice, for purposes of numerical calculation, a small number (~ 100) of R values is sufficient to provide necessary accuracy. The index n in Eq. (18) is the Born-Oppenheimer (BO) muonic wave-function designation. For the present work we are interested in the ground BO muonic state, designated by $1s\sigma$.

After dealing with the $\{\mathbf{r}\}$ part of the Hilbert space, the $\{\mathbf{R}\}$ part of the problem is treated next. One constructs the equation

$$[H^{\mathrm{sep}}+H^{\mathrm{ang}}+U(R)]\chi_\tau(\mathbf{R})=E_\tau\chi_\tau(\mathbf{R}) \tag{19}$$

in which the index τ stands for the set of quantum numbers L (total angular momentum excluding spin), M (z projection of L), and v (vibrational quantum number). There are typically two possible choices for the potential curve $U(R)$. One may set the potential curve equal to the BO potential curve obtained from Eq. (18),

$$U(R)=E_n^{\mathrm{BO}}(R)\ , \tag{20}$$

in which case one has the BO approximation. The second choice is to include the first-order diagonal corrections,

$$U(R)=E_n^{\mathrm{BO}}(R)+(\phi_n(\mathbf{r};R)\,|\,H^{\mathrm{sep}}+H^{\mathrm{ang}}+H^{\mathrm{mp}}\,|\,\phi_n(\mathbf{r};R))\ , \tag{21}$$

in which case one has the standard adiabatic (SA) approximation. The SA approximation requires knowledge of more matrix elements than the BO approximation, but leads to more accurate results.

Once the choice of potential curve has been made, it is a simple matter to solve Eq. (19) using standard techniques. The rotational symmetry of the problem allows separation of variables between the angular and radial degrees of freedom. The angular functions may be determined analytically and various numerical schemes exist for integrating the resulting radial differential equation. Once Eq. (19) is solved, the approximation to E in Eq. (17) is given by E_τ, while the approximation to $\Psi(\mathbf{r},\mathbf{R})$ is given by $\phi_n(\mathbf{r};R)\chi\tau(\mathbf{R})$.

An alternative method of implementing an adiabatic approximation is to partition the Hilbert space $\{\mathbf{r},\mathbf{R}\}$ of the problem into separate $\{\mathbf{r},\hat{\mathbf{R}}\}$ and $\{R\}$ spaces, where $\hat{\mathbf{R}}$ is the internuclear orientation vector and R is the scalar internuclear separation. Then the first stage of the procedure is carried out by solving the differential equation

$$(H^{\mathrm{BO}}+H^{\mathrm{ang}}+H^{\mathrm{mp}})\phi'_{n'}(\mathbf{r},\hat{\mathbf{R}};R)=E'_{n'}(R)\phi'_{n'}(\mathbf{r},\hat{\mathbf{R}};R) \tag{22}$$

on the Hilbert space $\{\mathbf{r},\hat{\mathbf{R}}\}$ for all values of the parameter R. Here, the index n' includes L and M in addition to the muonic wave-function designation. As before, we take $L=M=0$ and the muonic wave-function designation to be $1s\sigma$. For $L\neq 0$, the angular couplings in Eq. (22) may prevent the BO muonic designations from serving as useful labels. Having dealt with the $\{\mathbf{r},\hat{\mathbf{R}}\}$ part of the problem, the $\{R\}$ part is treated next. One constructs the equation

$$[H^{\mathrm{sep}}+U'(R)]\chi'_v(R)=E'_v\chi'_v(R)\ , \tag{23}$$

where the potential curve $U'(R)$ is given by

$$U'(R)=E'_{n'}(R)+(\phi'_{n'}(\mathbf{r},\hat{\mathbf{R}};R)\,|\,H^{\mathrm{sep}}\,|\,\phi'_{n'}(\mathbf{r},\hat{\mathbf{R}};R))\ . \tag{24}$$

This approach is called the improved adiabatic (IA) approximation. Equation (23) is a purely radial equation that can be solved using straightforward numerical integration techniques. The approximate energy and total wave function are given by E_v and $\phi_{n'}(\mathbf{r},\hat{\mathbf{R}};R)\chi_v(R)$, respectively. The IA approximation leads to more accurate results than both the BO and SA approximations.

In the present work, Schrödinger's equation outside the nuclear region has been solved using the BO, SA, and IA methods of approximation. The majority of the computational labor required for each of these approaches is in the construction of the potential curves [Eqs. (20), (21), and (24)]. The potential curve for the BO approximation for $dt\mu$ may be taken directly from previous work on HD^+ (Ref. 9). For the SA approximation, results from previous calculations on HD^+ may be used to construct the potential curve, after scaling the diagonal corrections by the appropriate ratio of the reduced masses. The potential curve for the IA approximation cannot be obtained from previous results and it was necessary to perform this calculation for the present work. The results obtained are listed in Table II. The computational method used for this calculation is that described in Ref. 9.

As an indication of the accuracy obtained from the various approaches, Table III contains energies obtained from the three adiabatic methods, along with the exact nonadiabatic results, where regular boundary conditions have been imposed for all the calculations. The details of the calculation with regular boundary conditions are discussed in Sec. IV. For the energies listed, it is seen that the SA approximation leads to energies which are better than an order of magnitude more accurate than the BO approximation. Going to the IA approximation

reduces the error in the energy by an additional factor of about 4 for the ground vibrational state and 3 for the first excited vibrational state.

B. Separable forms for $n\alpha\mu$

To describe the $n\alpha\mu$ channel at small $r_{n\alpha}$ we use the $(\mathbf{r}_{n\alpha},\mathbf{r}_{\mu})$ coordinates of Fig. 1 in which the muon has the same coordinates as in the $dt\mu$ channel. Then it can be shown analytically that, when $r_{n\alpha}$ is near the channel radius ($a_{n\alpha}=3$ fm), the muonic wave function differs completely negligibly from the muonic wave function at $r_{n\alpha}=0$ [i.e., the initial muonic wave function $\phi_{\mu}^{0}(\mathbf{r}_{\mu})$], regardless of the speed with which the nuclear reaction takes place relative to the muonic motion. Thus, the wave function in this vicinity,

$$\Psi=\psi_{n\alpha}^{+}(\mathbf{r}_{n\alpha})\phi_{\mu}^{0}(\mathbf{r}_{\mu}) ,$$

separates in the channel coordinates $(\mathbf{r}_{n\alpha},\mathbf{r}_{\mu})$, where the $n\alpha$ outgoing wave,

$$\psi_{n\alpha}^{+}(\mathbf{r}_{n\alpha})\propto h_{2}^{(1)}(k_{n\alpha}r_{n\alpha})Y_{2}(\hat{\mathbf{r}}_{n\alpha}) ,$$

is expressed in terms of the spherical Hankel function of the first kind and spherical harmonic for $l=2$ because the nuclear resonance gives D-wave reaction products. The invariance of the muonic wave function at the nuclear surface implies that no change in the muon energy occurs during the nuclear reaction, so that the channel momentum $k_{n\alpha}$ is related to the d-t relative energy $E_{dt}=E-E_{\mu}^{0}$ by the usual two-body energy-shell relation,

$$k_{n\alpha}^{2}=2M_{n\alpha}(E_{dt}+Q) ,$$

in which $Q=17.59$ MeV is the energy released in the $^{3}\mathrm{H}(d,n)^{4}\mathrm{He}$ reaction.

We emphasize that the above form of the $n\alpha\mu$ wave function is valid only at small $r_{n\alpha}$. For values of $r_{n\alpha}$ much larger than $a_{n\alpha}$ the potential would strongly couple states of this form. In general, since the neutron has no Coulomb interactions with the other particles, the $n\alpha\mu$ channel Hamiltonian separates in the $(\mathbf{r}_{n},\mathbf{r}_{\mu\alpha})$ coordinates of Fig. 1, and one must project the above wave function onto products of functions of the $\mathbf{r}_{n}$ and $\mathbf{r}_{\mu\alpha}$ coordinates in order to calculate asymptotic quantities like the sticking coefficients.

TABLE II. IA muonic potential curve $W^{\mathrm{IA}}(R)$ obtained for $dt\mu$. The $V(R)$ used in Eq. (28) for this adiabatic approximation is obtained from the relation $V(R)=W^{\mathrm{IA}}(R)+1/R$. Units are muonic atomic units (m.a.u.).

R	W^{IA}	R	W^{IA}
0.0	−1.954 103 9	5.5	−0.679 106 8
0.1	−1.931 961 5	6.0	−0.658 217 1
0.2	−1.882 730 1	6.5	−0.641 162 3
0.3	−1.822 218 3	7.0	−0.627 047 1
0.4	−1.758 860 5	7.5	−0.615 363 6
0.5	−1.695 139 8	8.0	−0.606 010 9
0.6	−1.633 724 2	8.5	−0.598 671 9
0.7	−1.575 668 0	9.0	−0.592 543 6
0.8	−1.520 820 2	9.5	−0.587 023 9
0.9	−1.469 432 9	10.0	−0.581 926 3
1.0	−1.421 381 3	10.5	−0.577 224 9
1.1	−1.376 487 4	11.0	−0.572 906 7
1.2	−1.334 540 3	11.5	−0.568 945 1
1.3	−1.295 322 7	12.0	−0.565 506 9
1.4	−1.258 623 2	12.5	−0.561 958 0
1.5	−1.224 241 8	13.0	−0.558 866 9
1.6	−1.191 993 0	13.5	−0.556 005 7
1.7	−1.161 706 7	14.0	−0.553 349 7
1.8	−1.133 227 4	14.5	−0.550 877 9
1.9	−1.106 414 0	15.0	−0.548 571 6
2.0	−1.081 138 7	15.5	−0.546 414 8
2.1	−1.057 285 4	16.0	−0.544 393 4
2.2	−1.034 749 2	16.5	−0.542 494 9
2.3	−1.013 434 9	17.0	−0.540 708 4
2.4	−0.993 256 2	17.5	−0.559 024 4
2.5	−0.974 134 6	18.0	−0.537 434 2
2.6	−0.955 998 9	18.5	−0.535 930 1
2.7	−0.938 784 0	19.0	−0.534 505 5
2.8	−0.922 430 8	19.5	−0.533 154 0
2.9	−0.906 884 9	20.0	−0.531 870 2
3.0	−0.892 096 9	20.5	−0.530 649 2
3.2	−0.864 616 0	21.0	−0.529 486 5
3.4	−0.839 666 1	21.5	−0.528 377 9
3.6	−0.816 973 5	22.0	−0.527 319 7
3.8	−0.796 303 4	22.5	−0.526 308 7
4.0	−0.777 452 6	23.0	−0.525 341 7
4.2	−0.760 244 3	23.5	−0.524 415 9
4.4	−0.744 522 7	24.0	−0.523 528 7
4.6	−0.730 149 7	24.5	−0.522 677 7
4.8	−0.717 001 7	25.0	−0.521 860 8
5.0	−0.704 967 1	∞	−0.481 854 4

IV. CALCULATION OF THE COMPLEX EIGENVALUE

If we limit our attention to the $L=0$ states associated with the $1s\sigma$ potential curve, $\phi_{1s\sigma}$ approaches the function $\phi_{\mu}^{0}(\mathbf{r}_{\mu})$ for small R, so that $\tilde{L}_{1}$ (Sec. III B) serves as a left-hand boundary value for the logarithmic derivative of the radial function $\eta=R\chi$. With the specification of the adiabatic potentials outside the nuclear region (Sec.

TABLE III. Eigenenergies for the $(v=0,L=0)$ and $(v=1,L=0)$ vibrational-rotational states obtained using regular boundary conditions with the Born-Oppenheimer (BO), standard adiabatic (SA), improved adiabatic (IA), and exact nonadiabatic (NA) approaches. Energies are given in muonic atomic units such that 1 m.a.u. $=2(m_{\mu}/m_{e})\mathrm{Ry}=5626.318$ eV.

	$E^{(v=0,\ L=0)}$	$E^{(v=1,\ L=0)}$
BO	−0.558 503 044 7	−0.507 760 071 3
SA	−0.537 267 817 4	−0.486 017 246 5
IA	−0.538 230 841 4	−0.487 398 600 1
NA[a]	−0.538 596 8	−0.488 065 3

[a]Reference 10.

III A) and the asymptotic outgoing-wave (which becomes exponentially decreasing for $\mathrm{Im}k_{dt}>0$) condition, the radial eigenvalue problem is completely defined. The fact that $\tilde{L}_1$ is a complex number means, in general, that the energy and radial wave functions which solve the eigenvalue problem are also complex valued. This section contains a description of the approach used here for determining the complex energies E_0 which satisfy the eigenvalue problem. Before considering the case of the energy-dependent complex-valued nuclear boundary condition, however, we will discuss the more usual problem of regular boundary conditions imposed at the origin on the solution to the radial equation.

A. Regular boundary conditions (conventional bound state)

The radial Schrödinger equation for the BO, SA, and IA approaches is given by

$$\left[-\frac{1}{2M_{dt}}\left[\frac{\partial^2}{\partial R^2}+\frac{2}{R}\frac{\partial}{\partial R}\right]+V(R)-E\right]\chi(R)=0\ , \tag{25}$$

where $V(R)$ is the potential curve appropriate for the particular choice of adiabatic approximation. Note for the states under consideration that centrifugal terms are absent and all three potential curves have the same generic asymptotic expansion for small R, i.e.,

$$V(R)=\frac{1}{R}+V_0^{\mathrm{origin}}+O(R^2)\quad(\text{as } R\to 0)\ , \tag{26}$$

where values of the constant V_0^{origin} are different for the BO, SA, and IA potential curves and are given in Table IV. These values are seen to approach more closely the μ-^{5}He ground-state energy, $E_\mu^0=-1.955\,885$ muonic atomic units (m.a.u.), as the adiabatic approximation is improved, and they were the numbers actually used in each case to shift the R-matrix eigenvalues E_λ in Eq. (6). For large R, the potential curves have the asymptotic expansion

$$V(R)=V_0^{\mathrm{asym}}+V_{-4}^{\mathrm{asym}}R^{-4}+O(R^{-6})\quad(\text{as } R\to\infty)\ , \tag{27}$$

with values of the constants V_0^{asym} and V_{-4}^{asym} for the three potential curves given in Table IV. It is convenient to simplify Eq. (25) by performing the transformation $\eta=R\chi$, resulting in

$$\left[-\frac{1}{2M_{dt}}\frac{\partial^2}{\partial R^2}+V(R)-E\right]\eta(R)=0\ . \tag{28}$$

The regular boundary condition (that usually imposed for physically realistic solutions) is just that $\eta(R=0)=0$ and for a bound state we also have that $\eta(R\to\infty)=0$. For bound states these two conditions are met simultaneously only for certain discrete values of the energy, which are the eigenvalues of the problem. Given Eqs. (26) and (28), one easily finds that the desired regular solution has the small-R asymptotic expansion given by

TABLE IV. Asymptotic parameters for the BO, SA, and IA potential curves of $dt\mu$. The BO results are the well-known analytical values (Ref. 9), while the SA and IA results have been obtained here from numerical calculations. V_0^{origin}, V_0^{asym}, and V_{-4}^{asym} are listed in the appropriate muonic atomic units.

	V_0^{origin}	V_0^{asym}	V_{-4}^{asym}
BO	−2.000 000 0	−0.500 000 0	−2.250
SA	−1.953 026 0	−0.476 513 3	−2.602
IA	−1.954 103 9	−0.481 854 4	−2.516

$$\eta(R)=a_0\{R+M_{dt}R^2+\tfrac{1}{3}[M_{dt}^2+M_{dt}(V_0^{\mathrm{origin}}-E)]R^3+\cdots\}\ . \tag{29}$$

Similarly, given Eqs. (27) and (28), the asymptotic expansion for large R, satisfying the condition $\eta(R\to\infty)=0$, is found to be

$$\eta(R)=b_0\left(1+\frac{\beta}{6\alpha}R^{-3}-\frac{\beta}{4\alpha^2}R^{-4}+\cdots\right)\exp(-\alpha R)\ , \tag{30}$$

where

$$\alpha=[2M_{dt}(V_0^{\mathrm{asym}}-E)]^{1/2}$$

and

$$\beta=2M_{dt}V_{-4}^{\mathrm{asym}}\ .$$

The numerical determination of the eigenenergies and eigenfunctions requires a choice for the radial integration range. The left endpoint $R_{\min}$ must be close enough to the origin such that Eq. (29) serves as a sufficiently accurate approximation to the exact solution for the purpose of imposing the boundary condition. A second constraint on the choice of left endpoint is that it is far enough away from the origin to avoid numerical problems arising from the Coulomb term in the potential $V(R)$. The left endpoint should be a compromise between maximizing the accuracy of Eq. (29) (the smaller $R_{\min}$ is, the better) while minimizing the numerical problems due to the Coulomb singularity (the larger $R_{\min}$ is, the better). If the optimum choice of left end point is still not adequate for the desired accuracy, the problem can be cured by additional numerical precision and more terms in the expansion of Eq. (29). The right end point $R_{\max}$ of the interval is chosen to be large enough such that Eq. (30) serves as a sufficiently exact approximation for the purpose of imposing the boundary condition. The potential curve is flat and well behaved for large R, so there are no numerical difficulties associated with taking $R_{\max}$ as large as is necessary.

The choice of the method of numerical solution to be taken here is motivated by the fact that the numerical integration is more stable when performed in the direction in which the potential curve is decreasing. Given the nature of the potential curves encountered in the present work, it is useful to partition the integration

range into the two intervals $[R_{min}, R_{match}]$ and $[R_{match}, R_{max}]$, where R_{match} is the internuclear separation at which the potential curve assumes its minimum. Then, given knowledge of the logarithmic derivative at R_{min} and some assumed value of the energy, E_{guess}, Eq. (28) can be integrated from R_{min} to R_{match}, yielding the logarithmic derivative at R_{match} for the left interval. Similarly, given knowledge of the logarithmic derivative at R_{max} and the same value of E_{guess}, Eq. (28) can be integrated from R_{max} to R_{match}, yielding the logarithmic derivative at R_{match} for the right interval. The eigenvalue condition for this problem is that the logarithmic derivative at R_{match} obtained from the left and right intervals are equal. The bound-state energy E_b for which this condition is satisfied can be obtained by iteration.

Having thus described the general approach of solving the eigenvalue problem with regular boundary conditions, only a few computational details remain to be considered. The numerical integration of Eq. (28) is fairly straightforward except in the region of the Coulomb singularity, where additional care must be taken. The difficulty arises because most numerical integration schemes require that the potential is approximately some simple polynomial (usually a constant) over the length of an integration step. This criterion can be satisfied closer to $R=0$ most simply by taking smaller steps. The integration region farther away from $R=0$ does not require such small steps; the additional operations required for the propagation in this region would lead to unnecessary computational expense and possibly poorer numerical results. These observations suggest that in the integration region where the Coulomb behavior is predominant, the numerical difficulty may be averted by choosing a variable step size which decreases with decreasing R. The choice taken here for the step size near the Coulomb singularity is $d_i=\alpha R_i$, where d_i is the ith step interval length, R_i is the value of R at the left end point of the ith interval, and α is an appropriate scale factor. Far enough away from the Coulomb singularity the step size is taken to be constant.

Using this procedure, solutions satisfying regular boundary conditions have been obtained by imposing the inner boundary condition from Eq. (29) at $R_{min}=0.01$ m.a.u. (muonic Bohr radii) and the outer boundary condition from Eq. (30) at $R_{max}=25.00$ m.a.u. These choices of R_{min} and R_{max} are sufficiently deep into their respective asymptotic regions such that Eqs. (29) and (30) provide adequate accuracy. The values of the potential curves required for the numerical integrations have been obtained by splining the values obtained from Ref. 9 (for BO and SA) and Table II of the present work (for IA).

Note that the energies in Tables III and V are listed to more digits than is warranted by the density and accuracy of the potential curve points (however, they *do* represent accurate solutions to the *given* potential curves). This has been done for the purpose of computing the shift in energies due to nuclear boundary conditions. One finds that the computed energy shift, calculated by taking the difference between the regular and nuclear boundary condition energies, is relatively insensitive to errors in the potential curve. In other words, potential curve inaccuracies tend to shift the regular and nuclear boundary-condition energies by essentially the same amount, so when the difference of the energies is taken the errors tend to cancel. Therefore the effect of boundary conditions can be obtained with potential curves of the present accuracy, as long as calculations are performed in a consistent manner.

B. Nuclear boundary conditions (resonance)

Calculations for the nuclear boundary-condition problem are performed using the same general approach as for the regular boundary-condition case. The only difference is that instead of Eq. (29) for the inner boundary condition we have the energy-dependent complex-valued boundary condition $\tilde{L}_1$ (described in Sec. II B) imposed at the d-t channel radius given by $R=0.019\,928$ m.a.u. ($=5.1$ fm). The nuclear logarithmic derivative $\tilde{L}_1$ is a relatively slowly-varying function of energy with a non-negligible imaginary part. Its value at the complex resonance energy (which is indistinguishable from its value at the molecular binding energy) differs significantly from the logarithmic derivative of the bound-state wave function, as will be seen below. As before, the outer boundary condition given by Eq. (30) is imposed at $R=25.00$ m.a.u.

The only additional complication posed by this problem is that the eigenfunction and eigenenergy will be complex valued, so the method of integration must allow complex arithmetic. Note that the variable-step-size approach must again be employed to handle problems due to the Coulomb nature of the potential curve for small R. The eigenvalue condition is the same as before, meaning that the complex-valued logarithmic derivatives at R_{match} obtained from the left and right intervals are

TABLE V. Complex eigenenergies for the $(v=0, L=0)$ and $(v=1, L=0)$ vibrational-rotational states obtained using nuclear boundary conditions with the BO, SA, and IA approaches. Energies are given in muonic atomic units.

	$E^{(v=0,\,L=0)}$	$E^{(v=1,\,L=0)}$
BO	$-0.558\,503\,220\,1-(9.20\times10^{-8})i$	$-0.507\,760\,206\,8-(7.13\times10^{-8})i$
SA	$-0.537\,267\,962\,2-(7.58\times10^{-8})i$	$-0.486\,017\,372\,3-(6.61\times10^{-8})i$
IA	$-0.538\,230\,985\,7-(7.55\times10^{-8})i$	$-0.487\,398\,720\,1-(6.31\times10^{-8})i$

equal. The complex energy E_0 for which this condition is satisfied can be obtained by iteration. The complex energies which solve the problem with the nuclear boundary condition are listed in Table V.

Having computed the eigenenergies with both regular and nuclear boundary conditions, it is now a simple matter to obtain the energy shift and resonance width due to the nuclear boundary condition. The energy shift ΔE is given by

$$\Delta E = \mathrm{Re}E_0 - E_b \ , \tag{31}$$

while the width of the resonance is, of course, $\Gamma = -2\,\mathrm{Im}E_0$. Values of the shifts and widths for the two vibrational levels considered are listed in Table VI, along with the results of Bogdanova *et al.*[4] Calculations performed using the three different choices of potential curve lead to results which indicate that the shifts and widths are relatively insensitive to the potential curve used.

It is interesting to note that, although the effect of the nuclear boundary condition on the eigenvalue is small, its effect on the small-distance behavior of the wave function is quite large. This can be seen from the numbers given in Table VII, which compares the logarithmic derivative of the IA molecular radial wave functions at the channel radius for the case of regular (bound-state) and nuclear (resonance) boundary conditions. Due to the rapid change of the *molecular* logarithmic derivative with energy (reflecting the large portion of the wave-function normalization that occurs in the channel region), however, the large change in logarithmic derivative is realized with a small displacement away from the binding energy in the complex energy plane.

V. CONCLUSION

We have calculated the effect of the nuclear region on the $L=0$ states of the $dt\mu$ molecule, in the approximation that the muonic and nuclear degrees of freedom separate at the nuclear surface, and that the $dt\mu$ wave function is described in the channel region by various adiabatic approximations. We find that the nuclear effects significantly change the small-distance behavior of the wave function and result in downward shifts of the binding energies and nonzero widths of the order of 1 meV, confirming results obtained earlier by Bogdanova *et al.*[4] Compared to those of Ref. 4, the shifts from our IA calculation, ΔE_{IA}, are about 15% smaller in magnitude, and the widths Γ_{IA} are about 4% larger. This is reasonable agreement, considering the different formulations and approximations used in the two calculations.

Bogdanova *et al.*[4] solve an integral equation, in which they construct the (principal-value) Green's function from a spectral expansion involving (in principle) all bound and continuum $dt\mu$ states. We solve a differential equation for only the $dt\mu$ state of interest, using boundary-matching techniques to find directly the complex eigenvalue that is a pole of the outgoing-wave Green's function, as is proper for resonances. Our approach, though more numerical in character, appears to be more direct, and involves fewer approximations than that of Ref. 4.

The parametrization of the nuclear amplitudes in Ref. 4 resembles a single-level Breit-Wigner form that takes proper account of the energy dependence of the d-t width and shift functions. Our multilevel R-matrix parametrization would reduce approximately to such a form at low energies. Although there is little correspondence between the parameters[4] of their fit and the resonance parameters[7] obtained from the four-level R-matrix fit, the nuclear amplitudes in both cases appear to have similar behavior, based on the Argand diagrams shown in Ref. 4. [However, our d-t scattering amplitude is shifted to the right with respect to theirs in Fig. 4(a) of Ref. 4, so that it intersects the origin at zero energy, as it should.]

Although the bound-state $dt\mu$ calculations were done nonadiabatically in Ref. 4, the eigenvalue calculations including nuclear effects used adiabatic approximations in the spectral expansion of the principal-value Green's function. Only the "dominant adiabatic component" of the wave function was retained in the summation over bound states, and the continuum-state solutions were obtained using a potential curve (i.e., adiabatically). It is not clear how to relate these adiabatic approximations to any of those that we have used, but we believe the differences in adiabatic approximation to be the main source of the modest discrepancy between our calculated eigenvalues and those of Bogdanova *et al.* To a lesser extent, differences in the nuclear amplitudes, and our using the outgoing-wave Green's function rather than the principal-value Green's function, contribute to the discrepancy.

The results obtained from the three adiabatic approximations used in this work provide a systematic examina-

TABLE VI. Energy shifts and resonance widths for the $(v=0, L=0)$ and $(v=1, L=0)$ vibrational-rotational states due to nuclear boundary conditions. Energies are given in units of 10^{-4} eV.

	$\Delta E^{(v=0,\,L=0)}$	$\Gamma^{(v=0,\,L=0)}$	$\Delta E^{(v=1,\,L=0)}$	$\Gamma^{(v=1,\,L=0)}$
BO	−9.87	10.35	−7.63	8.03
SA	−8.15	8.53	−7.08	7.44
IA	−8.12	8.50	−6.75	7.10
Ref. 4	−9.6	8.2	−8.0	6.8

TABLE VII. Logarithmic derivatives of the $(v=0, L=0)$ IA radial solution at the d-t channel radius ($R=0.019\,928$ m.a.u.) for regular (bound-state) and nuclear (resonance) boundary conditions.

	$R\frac{d\eta}{dR}\Big/\eta$ (dimensionless)	$\frac{d\eta}{dR}\Big/\eta$ (inverse m.a.u.)
Regular	1.1948	59.955
Nuclear ($=\tilde{L}_1$)	$-0.249\,56-0.096\,84i$	$-12.523-4.859i$

tion of the sensitivity of the shifts and widths to the accuracy of the approximation. For the $L=0$ ground vibrational state the SA approximation leads to significantly different results from that of the BO approximation, while the SA and IA results are quite close. For this state, the difference of the IA energy from the exact (nonadiabatic) energy is about one-fourth that of the SA energy; hence the IA wave function should be significantly more accurate than the SA wave function. Thus, the small variation in the shift and width when the appreciably more accurate IA wave function is used would appear to indicate that the complex eigenvalue has achieved good convergence with respect to the exact, nonadiabatic value. For the $L=0$ first excited vibrational state, there is a greater difference between the SA and IA results. A greater difference might be expected because this state is close to the dissociation limit and is therefore more affected by symmetry-breaking behavior (as described in Ref. 9), which is taken into account in the IA formulation, but not in the SA approach.

Based on the apparent convergence of the energy eigenvalues in Tables III and V toward the nonadiabatic values, we are led to extrapolate that the IA shifts and widths of Table VI are probably within a few percent of the exact results. Additionally, uncertainties of the order of 2% enter through the nuclear information, due to uncertainties in the $\frac{3}{2}^+R$-matrix parameters and to neglect of the $\frac{1}{2}^+$ transitions. We therefore estimate an overall uncertainty in the IA values of the shifts and widths of less than 10%.

ACKNOWLEDGMENT

This work was supported by the U.S. Department of Energy, in large part by the Division of Advanced Energy Projects.

[1]S. E. Jones *et al.*, Phys. Rev. Lett. **51**, 1757 (1983); **56**, 588 (1986); W. H. Breunlich *et al.*, *ibid.* **58**, 329 (1987).

[2]J. S. Cohen, Phys. Rev. Lett. **58**, 1407 (1987).

[3]L. N. Bogdanova, V. E. Markushin, V. S. Melezhik, and L. I. Ponomarev, Yad. Fiz. **34**, 1191 (1981) [Sov. J. Nucl. Phys. **34**, 662 (1981)].

[4]L. N. Bogdanova, V. E. Markushin, and V. S. Melezhik, Zh. Eksp. Teor. Fiz. **81**, 829 (1981) [Sov. Phys.—JETP **54**, 442 (1981)].

[5]E. P. Wigner and L. Eisenbud, Phys. Rev. **72**, 29 (1947); A. M. Lane and R. G. Thomas, Rev. Mod. Phys. **30**, 257 (1958).

[6]G. M. Hale and D. C. Dodder (to be published). Preliminary results are described in *Nuclear Cross Sections for Technology,* Natl. Bur. Stand. (U.S.) Spec. Publ. No. 594, edited by J. L. Fowler, C. H. Johnson, and C. D. Bowman (U.S. GPO Washington, D.C., 1980), p. 650.

[7]G. M. Hale, R. E. Brown, and N. Jarmie, Phys. Rev. Lett. **59**, 761 (1987).

[8]T. Teichmann and E. P. Wigner, Phys. Rev. **87**, 123 (1952). See also Lane and Thomas, Ref. 5.

[9]M. C. Struensee, J. S. Cohen, and R. T Pack, Phys. Rev. A **34**, 3605 (1986).

[10]C.-Y. Hu, Phys. Rev. A **36**, 4135 (1987).